

# Avoiding disentanglement of multipartite entangled optical beams with a correlated noisy channel

Xiaowei Deng,<sup>1,2</sup> Caixing Tian,<sup>1,2</sup> Xiaolong Su<sup>1,2\*</sup> and Changde Xie<sup>1,2</sup>

<sup>1</sup>State Key Laboratory of Quantum Optics and Quantum Optics Devices,

Institute of Opto-Electronics,

Shanxi University, Taiyuan 030006, China

<sup>2</sup>Collaborative Innovation Center of Extreme Optics,

Shanxi University, Taiyuan 030006, China

\*Corresponding author, e-mail: suxl@sxu.edu.cn

A quantum communication network can be constructed by distributing a multipartite entangled state to space-separated nodes. Entangled optical beams with highest flying speed and measurable brightness can be used as carriers to convey information in quantum communication networks. Losses and noises existing in real communication channels will reduce or even totally destroy entanglement. The phenomenon of disentanglement will result in the complete failure of quantum communication. Here, we present the experimental demonstrations on the disentanglement and the entanglement revival of tripartite entangled optical beams used in a quantum network. We discover that symmetric tripartite entangled optical beams are robust in pure lossy but noiseless channels. While in a noisy channel the excess noise will lead to the disentanglement and the destroyed entanglement can be revived by the use of a correlated noisy channel (non-Markovian environment). The presented results provide useful technical references for establishing quantum networks.

PACS numbers: 03.67.Hk, 03.65.Ud, 42.50.Ex, 42.50.Lc

## INTRODUCTION

Quantum entanglement is a fundamental resource in quantum information tasks [1]. Considerable progress has been made in quantum information processing with entangled optical beams because the manipulation and measurement of the quadrature amplitudes of optical field are familiar in classical communication and processing technologies [2–4]. The used quantum variables, amplitude and phase quadratures, are just the analogies of position and momentum of a particle [2]. Especially, the multipartite entangled state can be used to complete one-way quantum computation [5–8] and to construct quantum communication networks, such as quantum teleportation network [9, 10], controlled dense coding quantum communication [11], and wavelength-multiplexed quantum network with ultrafast frequency comb [12]. In quantum communication networks, quantum states carrying information are transmitted between space-separated nodes through quantum channels, while losses and noises in channels will unavoidably lead to decoherence of quantum states.

Decoherence, which is often caused by the interaction between system and the environment, is a main factor limiting the development of the quantum information technology. In quantum communication, the distributed entanglement will decrease because of the unavoidable decoherence in the quantum channel. In this case, entanglement purification, which is a way to distill highly entangled states from less entangled ones, is a necessary step to overcome decoherence [13–16]. Furthermore, it has been shown that decoherence will lead to entanglement sudden death (ESD) [17, 18], where two entangled qubits become completely disentangled in a

finite-time under the influence of vacuum. ESD for multipartite entangled states has also been discussed theoretically [19, 20]. Various methods to recover the bipartite entanglement after ESD occurred have been proposed and demonstrated during past several years, such as the non-Markovian environment [21], weak measurement [22], feedback [23], *et al.* The fidelity of quantum teleportation directly depends on the entanglement degree of utilized quantum resource. If disentanglement occurs in a quantum teleportation network, the fidelity will never exceed its classical limit and thus the quantum communication will fail. Thus, it is necessary to investigate the physical conditions of reducing and destroying multipartite entanglement in quantum channels and explore the feasible schemes of avoiding disentanglement.

Generally, there are two types of quantum channels, the lossy channel and the noisy channel. In a lossy but noiseless (without excess noise) quantum channel, the noise induced by loss is nothing but the vacuum noise (corresponding to a zero-temperature environment) [4]. In a noisy channel, the excess noise higher than the vacuum noise exists [4]. It has been shown that the bipartite Gaussian entangled optical beams can be robust against loss [24], while the three-color entanglement among three asymmetric optical modes can be fragile against loss, which means that the disentanglement is observed in a lossy channel, at some situation [25]. We theoretically analyze the physical condition of the robustness for tripartite entangled optical beams over lossy channels, and experimentally demonstrate that the symmetric tripartite entangled state is robust against loss in quantum channels.

The excess noise in a communication channel is another main factor limiting the transmission of informa-

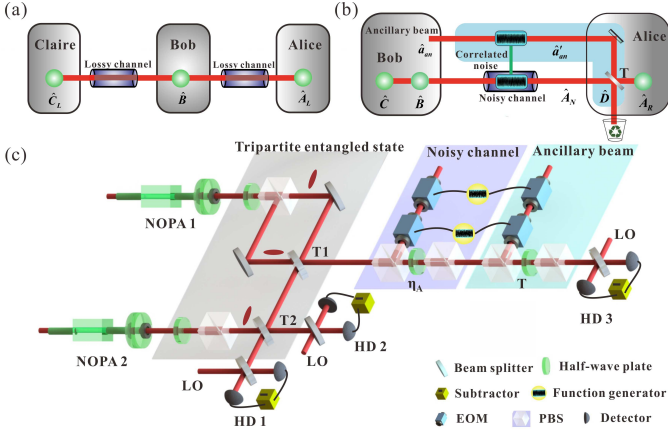


FIG. 1: **Schematic of principle and experimental setup.** (a) Two modes ( $\hat{A}$  and  $\hat{C}$ ) of a tripartite entangled state are distributed over two lossy quantum channels to Alice and Claire, respectively. (b) One mode of the tripartite entangled state is distributed over a noisy channel, where disentanglement is observed among optical modes  $\hat{A}_N$ ,  $\hat{B}$  and  $\hat{C}$ . The entanglement revival operation is implemented by coupling an ancillary beam ( $\hat{a}'_{an}$ ) who has correlated noise with the environment with the transmitted mode  $\hat{A}_N$  on a beam-splitter with transmission efficiency of  $T$ , thus the entanglement among modes  $\hat{A}_R$ ,  $\hat{B}$  and  $\hat{C}$  is revived. (c) The schematic of experimental set-up for distributing a mode of the tripartite entangled optical beams over a noisy channel and the entanglement revival. T1 and T2 are the beam splitters used to generate the GHZ entangled state.  $\eta_A$  and  $T$  are the transmission efficiencies of the noisy channel and the revival beam-splitter, respectively. HD1 – 3, homodyne detectors. LO, the local oscillator.

tion, for example, it will decrease the secure transmission distance of quantum key distribution [4]. The noises in today's communication systems exhibit correlations in time and space, thus it will be relevant to consider channels with correlated noise (non-Markovian environment) [26–28]. A correlated noisy channel has been used to complete Gaussian error correction [28] and to protect squeezing in quantum communication with squeezed state over a noisy quantum channel, in which the disentanglement is observed. By applying an ancillary optical beam and establishing a correlated noisy channel, we successfully avoid disentanglement among the tripartite disentangled optical beams.

### Experimental scheme

The quantum state used in the experiment is a continuous variable Greenberger-Horne-Zeilinger (GHZ) tripartite entangled state [10, 11], which is prepared deterministically. The correlation variances between the amplitude (position) and phase (momentum) quadra-

tures of the tripartite entangled state are expressed by  $\Delta^2(\hat{x}_A - \hat{x}_B) = \Delta^2(\hat{x}_A - \hat{x}_C) = \Delta^2(\hat{x}_B - \hat{x}_C) = 2e^{-2r}$  and  $\Delta^2(\hat{p}_A + \hat{p}_B + \hat{p}_C) = 3e^{-2r}$ , respectively, where the subscripts correspond to different optical modes ( $\hat{A}$ ,  $\hat{B}$  and  $\hat{C}$ ) and  $r$  is the squeezing parameter ( $r = 0$  and  $r = +\infty$  correspond to no squeezing and the ideally perfect squeezing, respectively). Obviously, in the ideal case with infinite squeezing ( $r \rightarrow \infty$ ), these correlation variances will vanish and the better the squeezing, the smaller the noise terms.

When two optical modes ( $\hat{A}$  and  $\hat{C}$ ) of a tripartite entangled state are distributed by Bob (who retains mode  $\hat{B}$ ) to two nodes (Alice and Claire) over two lossy channels, a quantum network with three users Alice, Bob and Claire is established [Fig. 1(a)]. After the transmission of optical modes  $\hat{A}$  and  $\hat{C}$  over two lossy channels, the output modes are given by  $\hat{A}_L = \sqrt{\eta_A}\hat{A} + \sqrt{1-\eta_A}\hat{v}_A$  and  $\hat{C}_L = \sqrt{\eta_C}\hat{C} + \sqrt{1-\eta_C}\hat{v}_C$ , where  $\eta_{A(C)}$  and  $\hat{v}_{A(C)}$  represent the transmission efficiency of the quantum channel and the vacuum state induced by loss into the quantum channel, respectively. When  $\eta_A \neq 1, \eta_C = 1$ , it corresponds to the situation that the optical mode  $\hat{A}$  is distributed over a lossy channel to another node while modes  $\hat{B}$  and  $\hat{C}$  are maintained in a node. While when mode  $\hat{A}$  is distributed over a noisy channel [Fig. 1(b)], the transmitted mode is expressed by

$$\hat{A}_N = \sqrt{\eta_A}\hat{A} + \sqrt{1-\eta_A}\hat{v}_A + \sqrt{(1-\eta_A)g_a}\hat{N}, \quad (1)$$

where  $\hat{N}$  and  $g_a$  represent the Gaussian noise in the channel and the magnitude of noise, respectively. The excess noise on the transmitted mode will possibly lead to the disentanglement of the tripartite entangled state. In order to avoid disentanglement of the tripartite entangled state, an ancillary beam with correlated noise and a revival beam-splitter with the transmission coefficient  $T$  are used. The ancillary beam carrying correlated noise is expressed by  $\hat{a}'_{an} = \hat{a}_{an} + \sqrt{g_b}\hat{N}$ , where  $\hat{a}_{an}$  is the ancillary beam and  $g_b$  describes the magnitude of the correlated noise, which is an adjustable parameter in experiments. The transmitted ( $\hat{A}_R$ ) and reflected ( $\hat{D}$ ) beams from the revival beam-splitter are  $\hat{A}_R = \sqrt{\eta_A T}\hat{A} + \sqrt{(1-\eta_A)T}\hat{v}_A - \sqrt{1-T}\hat{a}_{an} + (\sqrt{(1-\eta_A)g_a T} - \sqrt{(1-T)g_b})\hat{N}$  and  $\hat{D} = \sqrt{\eta_A(1-T)}\hat{A} + (\sqrt{(1-\eta_A)(1-T)g_a} + \sqrt{Tg_b})\hat{N} + \sqrt{(1-\eta_A)(1-T)}\hat{v}_A + \sqrt{T}\hat{a}_{an}$ , respectively. If the values of  $g_b$  and  $T$  are chosen to satisfy the following expression

$$\frac{g_a}{g_b} = \frac{1-T}{(1-\eta_A)T}, \quad (2)$$

the noise on the output mode  $\hat{A}_R$  will be removed totally. In this case, the output mode becomes

$$\hat{A}_R = \sqrt{\eta_A T}\hat{A} + \sqrt{(1-\eta_A)T}\hat{v}_A - \sqrt{1-T}\hat{a}_{an}, \quad (3)$$

which is immune from the excess noise. The excess noise is transferred onto the reflected beam  $\hat{D}$  (which is aban-

done) due to the use of the beam-splitter. Thus the tripartite entanglement among  $\hat{A}_R$ ,  $\hat{B}$  and  $\hat{C}$  is preserved by using a correlated noisy channel.

### Experimental set-up

The experimental set-up for distributing a mode of the tripartite entangled optical beams over a noisy channel and the entanglement revival is shown in Fig. 1(c). The nondegenerate optical parametric amplifiers (NOPAs) are pumped by a common laser source, which is a continuous wave intracavity frequency-doubled and frequency-stabilized Nd:YAP/LBO (Nd-doped YAlO<sub>3</sub> perovskite/lithium triborate) laser. Each of the NOPAs consists of an  $\alpha$ -cut type-II KTP crystal and a concave mirror. The front face of the KTP crystal was coated to be used for the input coupler and the concave mirror serves as the output coupler of the squeezed states. The transmissions of the input coupler at 540 nm and 1080 nm are 99.8% and 0.04%, respectively. The transmissions of the output coupler at 540 nm and 1080 nm are 0.5% and 5.2%, respectively. A pair of  $\hat{x}$ -squeezed and  $\hat{p}$ -squeezed states in two orthogonal polarizations are produced by NOPA1 [30]. The other  $\hat{x}$ -squeezed state is produced by NOPA2. NOPAs are locked individually by using Pound-Drever-Hall method with a phase modulation of 56 MHz on 1080 nm laser beam [31]. Both NOPAs are operated at deamplification condition, which corresponds to lock the relative phase between the pump laser and the injected signal to  $(2n+1)\pi$  ( $n$  is the integer).

The tripartite entangled state of optical field at the sideband frequency of 2 MHz is obtained by combining three squeezed states of light with  $-3.5$  dB squeezing and 8.5 dB anti-squeezing on two optical beam-splitters with transmission coefficients  $T_1 = 1/3$  and  $T_2 = 1/2$ , respectively [see APPENDIX A]. For a real communication channel, the loss and noise are coming from the environment as that shown in Fig. 1. The loss in the quantum channel is mimicked by a beam-splitter composed by two polarization beam-splitters (PBSs) and a half-wave plate placed between them. The noisy channel is simulated by adding a Gaussian noise on a coherent beam with electro-optic modulators (EOMs) and then the modulated beam is coupled with the transmitted mode on a beam-splitter with transmission efficiency  $\eta_A$ . When an ancillary beam with the correlated noise is mixed with the transmitted mode on a beam-splitter of the transmission coefficient  $T$ , the entanglement revival is completed. The covariance matrix of the output state is measured by three homodyne detectors. The quantum efficiency of the photodiodes used in the homodyne detectors are 95%. The interference efficiency on all beam-splitters are about 99%.

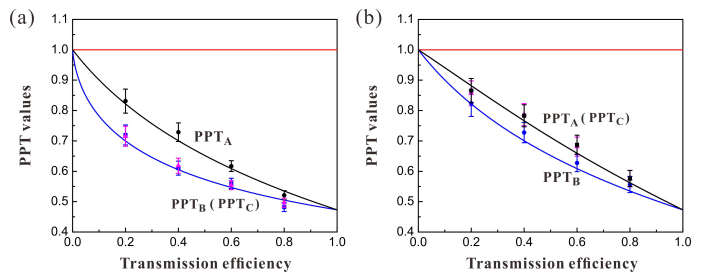


FIG. 2: **The entanglement in lossy channels.** (a) One optical mode  $\hat{A}$  is distributed in the lossy channel ( $\eta_A \neq 1$ ,  $\eta_C = 1$ ). (b) Two optical modes  $\hat{A}$  and  $\hat{C}$  are distributed in the lossy channels with the same transmission efficiency ( $\eta_A \neq 1$ ,  $\eta_C \neq 1$ ). PPT values are all below the entanglement boundary (red lines), which means that the tripartite entanglement is robust against loss in quantum channels. The black, blue and pink dots represent the experimental data for different PPT values, respectively. Error bars represent  $\pm$  one standard deviation and are obtained based on the statistics of the measured noise variances.

### The positive partial transposition criterion

The positive partial transposition (PPT) criterion [32, 33] is a necessary and sufficient condition for judging the existence of quantum entanglement among  $N$  Gaussian optical beams, when the state has the form of bipartite splitting with only a single mode on one side like  $(1|N-1)$  [34, 35]. We use the PPT criterion to verify the disentanglement and the entanglement revival of the tripartite entangled states of light. Based on above-mentioned expressions of output state, we obtain the covariance matrix, which is given in APPENDIX B, and calculate the symplectic eigenvalues. The positivity is checked by evaluating the symplectic eigenvalues of the partially transposed matrix and the state is separable if any of the symplectic eigenvalues is larger than or equal to 1 [36].

At the level of quadrature operators, the partial transposition with respect to mode  $k$  ( $k = 1, 2, 3$ ) corresponds to the change of sign of the phase quadrature, i. e.  $\hat{p}_k \rightarrow -\hat{p}_k$ . Symplectic eigenvalues of covariance matrix are defined as the positive roots of the polynomial  $|\gamma^{T(k)} - i\mu\Omega| = 0$ , where  $|A|$  denotes the determinant of matrix [36].  $\gamma^{T(k)} = T_k\gamma T_k^T$  is the partially transposed matrix of the quantum state, where  $T_k$  is a diagonal matrix with all diagonal elements equal to 1 except for  $T_{2k,2k} = -1$ , and

$$\Omega = \bigoplus_{k=1}^3 \begin{pmatrix} 0 & 1 \\ -1 & 0 \end{pmatrix}. \quad (4)$$

We consider a bipartite splitting of a three-mode Gaussian state with covariance matrix  $\gamma$  such that one party holds mode  $k$  and the other party possesses the remained two modes. If the smallest symplectic eigenvalue  $\mu_k$  obtained from the polynomial is smaller than 1, the state

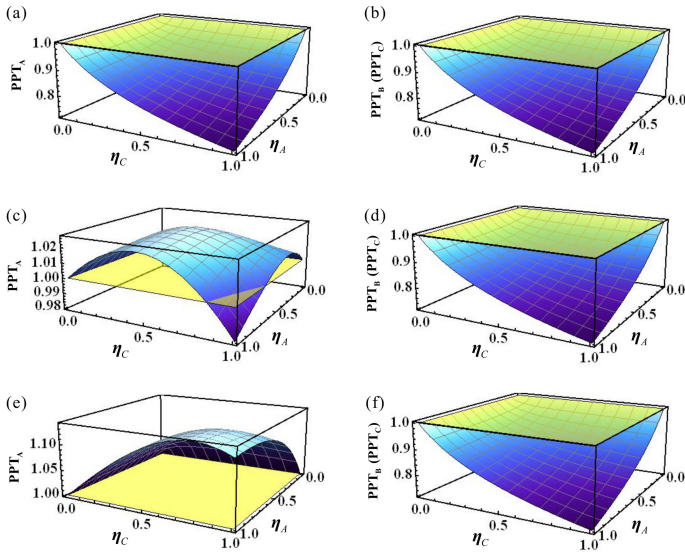


FIG. 3: **The entanglement properties of different asymmetric tripartite states in two lossy channels.** (a,b) PPT values of fully robust entanglement against loss with  $c_x/c = 0.8$ . (c,d) PPT values of a one-mode fragile state in lossy channels for attenuations with  $c_x/c = 0.5$ . (e,f) a totally one-mode biseparable state in lossy channels with  $c_x/c = 0.3$ .

is inseparable with respect to the  $k|ij$  splitting.

### Entanglement in lossy channels

Figure 2 shows that the tripartite entanglement is robust against loss in lossy quantum channels. The PPT values  $PPT_A$ ,  $PPT_B$  and  $PPT_C$  represent the different splittings for the  $(A|BC)$ ,  $(B|AC)$  and  $(C|AB)$ , respectively. The PPT values of distributing one optical mode ( $\hat{A}$ ) and two optical modes ( $\hat{A}$  and  $\hat{C}$ ) in one and two lossy channels (for simplification, we assume the losses in two quantum channels are the same) are shown in Fig. 2(a) and Fig. 2(b), respectively. The values of  $PPT_B$  and  $PPT_C$  in Fig. 2(a) [ $PPT_A$  and  $PPT_C$  in Fig. 2(b)] are the same because that the optical modes of the tripartite entangled state are symmetric and modes  $\hat{B}$  and  $\hat{C}$  do not interact with the environment (modes  $\hat{A}$  and  $\hat{C}$  are transmitted with the same transmission efficiency). Comparing the corresponding PPT values in Fig. 2(a) and Fig. 2(b), we can see that the tripartite entanglement is more robust if only a mode ( $\hat{A}$ ) pass through the lossy channel than that both modes  $\hat{A}$  and  $\hat{C}$  subject to the lossy channels, i. e. the degradation of entanglement in the case of  $\eta_C = 1$  is less than that in the case of  $\eta_A \neq 1$  and  $\eta_C \neq 1$ . In lossy channels, the tripartite entanglement gradually decreases along with the degradation of the transmission efficiency of quantum channel and finally tends to zero when the channel efficiency

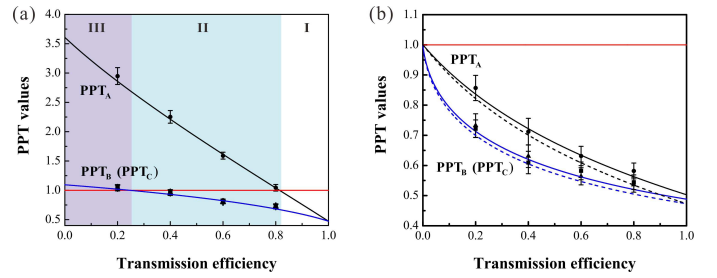


FIG. 4: **The disentanglement and entanglement revival in a noisy channel.** (a) The PPT values for the transmission in a noisy channel, where the variance of the excess noise is taken as five times of shot noise level. The tripartite entangled state experiences entanglement (I), one-mode biseparable (II) and fully disentanglement (III) along with the decreasing of the channel efficiency. (b) The PPT values after entanglement revival. Dash lines are the corresponding results of the perfectly revival, the results are the same with the lines in Fig. 2(a) which are obtained before disentanglement. The black dots represent the experimental data. Error bars represent  $\pm$  one standard deviation and are obtained based on the statistics of the measured noise variances.

equals to zero. This is different from the results in Ref. [25], where the disentanglement of a tripartite entangled light beam is observed over a lossy channel. We theoretically analyse the physical reason of the difference based on the covariance matrix and discover that it is because the tripartite entangled state prepared by us is a symmetric entangled state, while the state in Ref. [25] is an asymmetric state since the effect of the classical phonon noise, which are discussed detailedly at next section.

### Discussion on symmetric and asymmetric states

We consider the case of the transmission in two lossy channels for tripartite Gaussian symmetric and asymmetric optical states, respectively. For convenience, the covariance matrix of the original tripartite Gaussian state is written in terms of two-by-two submatrices as

$$\sigma = \begin{bmatrix} \sigma_A & \sigma_{AB} & \sigma_{AC} \\ \sigma_{AB}^T & \sigma_B & \sigma_{BC} \\ \sigma_{AC}^T & \sigma_{BC}^T & \sigma_C \end{bmatrix}, \quad (5)$$

in which each diagonal block  $\sigma_k$  is the local covariance matrix corresponding to the reduced state of mode  $k$  ( $k = A, B, C$ ), respectively, and the off-diagonal matrices  $\sigma_{mn}$  are the intermodal correlations between subsystems  $m$  and  $n$ . The detailed expressions of  $\sigma_k$  and  $\sigma_{mn}$  are given in APPENDIX B.

*Type I symmetric state.* If a quantum state has symmetric modes ( $\sigma_A = \sigma_B = \sigma_C$ ) and balanced correlations between subsystems  $\sigma_{mn}$ , i. e. the absolute values of main diagonal elements in  $\sigma_{mn}$  are the same, we say it is a symmetric state, where the variances are  $\Delta^2 \hat{x}_A =$

$\Delta^2 \hat{x}_B = \Delta^2 \hat{x}_C = s$ ,  $\Delta^2 \hat{p}_A = \Delta^2 \hat{p}_B = \Delta^2 \hat{p}_C = t$ ,  $\langle \delta \hat{x}_A \delta \hat{x}_B \rangle = \langle \delta \hat{x}_A \delta \hat{x}_C \rangle = \langle \delta \hat{x}_B \delta \hat{x}_C \rangle = c$ ,  $\langle \delta \hat{p}_A \delta \hat{p}_B \rangle = \langle \delta \hat{p}_A \delta \hat{p}_C \rangle = \langle \delta \hat{p}_B \delta \hat{p}_C \rangle = -c$ , and  $\langle \delta \hat{x}_j \delta \hat{x}_{j'} \rangle = 0$ . The corresponding covariance matrix is

$$\sigma_I = \begin{bmatrix} s & 0 & c & 0 & c & 0 \\ 0 & t & 0 & -c & 0 & -c \\ c & 0 & s & 0 & c & 0 \\ 0 & -c & 0 & t & 0 & -c \\ c & 0 & c & 0 & s & 0 \\ 0 & -c & 0 & -c & 0 & t \end{bmatrix}. \quad (6)$$

This type of quantum state can be generated by the interference of three squeezed states on beam-splitter network. The three squeezed states are produced from three NOPAs operating below its oscillation threshold, respectively [30]. The experimental values of parameters  $c$ ,  $s$  and  $t$  in Eq. (6) are obtained by the covariance matrix of the entangled state prepared by us [see Eq. (13) in APPENDIX B]. Apparently, the prepared state is a symmetric state. According to the theoretical calculation result shown in Fig. 2, in which all used parameters in the calculation are derived from Eq. (13) and (14) in APPENDIX B, it is proved that the symmetric quantum states are fully robust against losses in the two lossy channels.

*Type II asymmetric state.* The asymmetric quantum state has unbalanced correlations between subsystems ( $c_x \neq c$ ), whose covariance matrix is given by

$$\sigma_{II} = \begin{bmatrix} s & 0 & c_x & 0 & c_x & 0 \\ 0 & t & 0 & -c & 0 & -c \\ c_x & 0 & s & 0 & c & 0 \\ 0 & -c & 0 & t & 0 & -c \\ c_x & 0 & c & 0 & s & 0 \\ 0 & -c & 0 & -c & 0 & t \end{bmatrix}. \quad (7)$$

The entanglement property of the asymmetric state is shown in Fig. 3 [all parameters used in the calculation are also taken from Eq. (13) and (14) in APPENDIX B]. The mathematic operation of modifying a parameter,  $c_x$ , and keeping other elements in the covariance matrix unchanging is equivalent to physically add an uncorrelated noise into the generation system of the tripartite entangled state [37]. For example, the phonon noise in the prepared three-color entangled state in Ref. [25], which is produced by a non-degenerated optical parametric oscillator (NOPO) operating above its oscillation threshold, is a type of classical and uncorrelated noises. In an above-threshold NOPO, the effect of the uncorrelated phonon noise is large and thus the produced three-color entangled state is asymmetric [25]. In Eq. (7), we assume that the different amounts of the uncorrelated noise exist in mode  $\hat{A}$ , thus  $c_x$  in both  $\sigma_{AB}$  and  $\sigma_{AC}$  is changed simultaneously, while  $\sigma_{BC}$  is unchanged because it is not related to mode  $\hat{A}$ . Fig. 3(a) and 3(b) are the PPT values corresponding to  $c_x/c = 0.8$ , which show that the disentanglement never happens, thus the original state is robust against losses. Actually, all asymmetric states

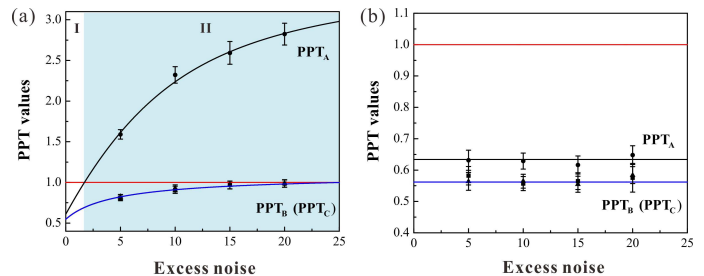


FIG. 5: **The disentanglement and revival of entanglement at different noise levels (in the unit of shot noise level).** (a) Disentanglement at different excess noise levels. (b) The PPT values after entanglement revival, and it is independent on the excess noise. The black dots represent the experimental data. Error bars represent  $\pm$  one standard deviation and are obtained based on the statistics of the measured noise variances.

correspond to  $c_x/c > 0.8$  are robust against losses according to our calculation. Fig. 3(c) and 3(d) are the PPT values corresponding to  $c_x/c = 0.5$ , which show that the disentanglement happens for A|BC during decreasing the transmission efficiencies, thus the original state is a one-mode fragile state for the attenuations. From Fig. 3(e) and 3(f) we can see that the state is a totally one-mode biseparable state when  $c_x/c = 0.3$ . Thus the original asymmetric tripartite state evolves from a robust state to a fully one-mode biseparable state with the decrease of the  $c_x$  value. We should emphase that that the asymmetric property of quantum states does not certainly result in the disentanglement, and only when the uncorrelated noise in the quantum state is large enough the disentanglement occurs. To the physical reason, the correlation among subsystems in a symmetric state is balanced, i. e. there is no uncorrelated noise in the quantum state. Thus all entangled modes for the symmetric state are equivalent and the entanglement is reduced gradually and continually in a lossy channel. However, for an asymmetric state, the correlation among subsystems is unbalanced, i. e. uncorrelated noises are added into the quantum state, which lead to disentanglement of the asymmetric tripartite state.

### Entanglement in noisy channel

When there is the excess noise in the quantum channel, the disentanglement is observed as shown in Fig. 4, where the variance of the excess noise is taken as five times of shot noise level and  $g_a = 1$ . The values of  $PPT_B$  and  $PPT_C$  are the same because the tripartite entangled state is symmetric and both modes  $\hat{B}$  and  $\hat{C}$  are retained in a node. In this case, we can assume that modes  $\hat{B}$  and  $\hat{C}$  have no interaction with the environment. Entanglement survives when the transmission efficiency satisfies  $0.81 < \eta \leq 1$  [region I in Fig. 4(a)]. When  $0.24 < \eta \leq 0.81$ ,

$PPT_A$  is above 1 while  $PPT_B$  and  $PPT_C$  are below 1, the state is corresponding to a one-mode biseparable state [region II in Fig. 4(a)], which means that mode  $\hat{A}$  is separated from modes  $\hat{B}$  and  $\hat{C}$ . When the transmission efficiency is  $\eta \leq 0.24$ , fully disentanglement is observed [region III in Fig. 4(a)], which will result in that the quantum communication between any two users is not possible to be implemented.

There are two adjustable parameters in the entanglement revival procedure,  $g_b$  and  $T$ . For different channel efficiency, we may fix one of them and adjust the other one to recover the entanglement according to Eq. (2). In the experiment, we chose to fix  $T$  and adjust  $g_b$  for different transmission efficiencies of the quantum channel. Generally,  $T$  can not be taken too small because it corresponds to add a linear loss on the transmitted mode, which will degrade the tripartite entanglement. The solid and dash lines in Fig. 4(b) represent the revived entanglement in our experiment with  $T = 90\%$  and in the ideal case with the perfectly revival, respectively. The imperfect transmission efficiency of the revival beam-splitter leads to the small difference between the two results. The parameters  $g_a/g_b$  are chosen to be 0.14, 0.18, 0.28 and 0.56 for channel efficiencies of 0.2, 0.4, 0.6 and 0.8, respectively. Fig. 4(b) shows that the entanglement is revived after the revival operation.

The dependence of entanglement on the excess noise is shown in Fig. 5, where the transmission efficiency is chosen to be 0.6,  $g_a/g_b = 0.28$ , and  $T = 90\%$ . We can see that the boundary of disentanglement depends on the excess noise level. When the variance of the excess noise is lower than 2.2 times of shot noise level for the transmission efficiency of  $\eta = 0.6$ , the entanglement can be survived in a noisy channel. When the variance of the excess noise is higher than 2.2 times of shot noise level for the transmission efficiency  $\eta = 0.6$ , the disentanglement happens and the state is reduced to an one-mode biseparable state [region II in Fig. 5(a)]. After the revival operation, the entanglement is recovered and it is independent on the excess noise as that indicated by Eq. (3).

## Discussion

In summary, we deeply investigate the different effects of the lossy channel and the noisy channel on the tripartite entangled state of light when it is distributed in a quantum network and point out that the entangled optical beams with the symmetric structure is more robust to the channel losses than that with the asymmetric structure. From the experimental and the calculated results we can conclude that the symmetry is a sufficient but not necessary condition for robustness of tripartite entanglement in a lossy channel. While for the asymmetric state, the robustness of the state depends on the correlation between subsystems.

Disentanglement is observed when the excess noise ex-

ists in the quantum channel. The symmetric tripartite entangled state is fragile against the excess noise, while it is robust against the pure loss. By creating a correlated noisy channel (non-Markovian environment), entanglement of the tripartite entangled state is preserved, thus disentanglement can be avoided with the correlated noisy channel. But when the revived state passed through a noisy channel again the disentanglement will possibly appear again.

The influence of loss and noise in quantum channel to the entanglement depends on the strength of them. The more the strength is, the large the influence is. The correlated noisy channel used in our experiment can only remove the effect of noise in the quantum channel, while the influence of loss can not be eliminated by the scheme. Fortunately, another technology, the noiseless linear amplification, can be used to eliminate the effect of loss on entanglement [38–41]. Due to that the disentanglement induced by environment is a specific phenomenon among correlated quantum systems, which is never observed in the studies of dissipation effects for classical systems, the presented results are significant to understand the dynamic behavior of the interaction of entangled states and different environment. Besides, our investigation also provides concrete references for establishing quantum network with multipartite entangled states of light.

**Acknowledgements** This research was supported by NSFC (Grant Nos. 11522433, 61475092) and OIT (2013805). X. Su and C. Xie conceived the original idea. X. Deng and X. Su designed the experiment. X. Deng, C. Tian and X. Su constructed and performed the experiment. X. Deng and C. Tian accomplished theoretical calculation. X. Deng, C. Tian and X. Su, accomplished the data analyses. X. Su and C. Xie wrote the paper.

## APPENDIX

### A. Preparation of the tripartite entangled state

The tripartite entangled state used in the experiment is a continuous variable tripartite Greenberger-Horne-Zeilinger (GHZ) state of optical field [9] which is prepared by coupling a phase-squeezed state ( $\hat{a}_2$ ) of light and two amplitude-squeezed states of light ( $\hat{a}_1$  and  $\hat{a}_3$ ) on an optical beam-splitter network, which consists of two optical beam-splitters with transmittance of  $T_1 = 1/3$  and  $T_2 = 1/2$ , respectively, as shown in Fig. 6. Three input squeezed states are expressed by

$$\begin{aligned}\hat{a}_1 &= e^{-r_1} \hat{x}_1^{(0)} + i e^{r_1} \hat{p}_1^{(0)}, \\ \hat{a}_2 &= e^{r_2} \hat{x}_2^{(0)} + i e^{-r_2} \hat{p}_2^{(0)}, \\ \hat{a}_3 &= e^{-r_3} \hat{x}_3^{(0)} + i e^{r_3} \hat{p}_3^{(0)},\end{aligned}\quad (8)$$

where  $r_i$  ( $i = 1, 2, 3$ ) is the squeezing parameter,  $\hat{x} = \hat{a} + \hat{a}^\dagger$  and  $\hat{p} = (\hat{a} - \hat{a}^\dagger)/i$  are the amplitude and phase

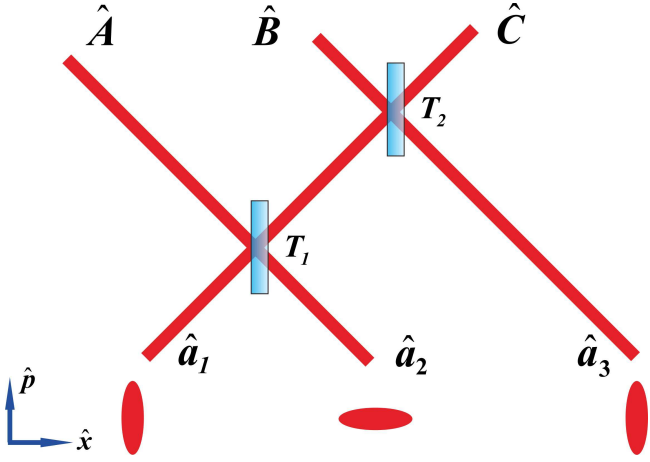


FIG. 6: The schematic of generation system of the tripartite entangled state.

quadratures of an optical field  $\hat{a}$ , respectively, and the superscript of the amplitude and phase quadratures represent the vacuum state. The transformation matrix of the beam-splitter network is given by

$$U = \begin{bmatrix} \sqrt{\frac{2}{3}} & \sqrt{\frac{1}{3}} & 0 \\ -\sqrt{\frac{1}{6}} & \sqrt{\frac{1}{3}} & \sqrt{\frac{1}{2}} \\ -\sqrt{\frac{1}{6}} & \sqrt{\frac{1}{3}} & -\sqrt{\frac{1}{2}} \end{bmatrix}, \quad (9)$$

the unitary matrix can be decomposed into a beam-splitter network  $U = B_{23}^+(T_2)I_2(-1)B_{12}^+(T_1)$ , where  $B_{kl}^+(T_j)$  stands for the linearly optical transformation on  $j$ th beam-splitter with transmission of  $T_j$  ( $j = 1, 2$ ), where  $(B_{kl}^+)_{kk} = \sqrt{1-T}$ ,  $(B_{kl}^+)_{kl} = (B_{kl}^+)_{lk} = \sqrt{T}$ ,  $(B_{kl}^+)_{ll} = -\sqrt{1-T}$ , are matrix elements of the beam-splitter.  $I_k(-1) = e^{i\pi}$  corresponds to a  $180^\circ$  rotation in phase space. The output modes from the optical beam-splitter network are expressed by

$$\begin{aligned} \hat{A} &= \sqrt{\frac{2}{3}}\hat{a}_1 + \sqrt{\frac{1}{3}}\hat{a}_2, \\ \hat{B} &= -\sqrt{\frac{1}{6}}\hat{a}_1 + \sqrt{\frac{1}{3}}\hat{a}_2 + \sqrt{\frac{1}{2}}\hat{a}_3, \\ \hat{C} &= -\sqrt{\frac{1}{6}}\hat{a}_1 + \sqrt{\frac{1}{3}}\hat{a}_2 - \sqrt{\frac{1}{2}}\hat{a}_3, \end{aligned} \quad (10)$$

respectively. Here, we have assumed that three squeezed states have the identical squeezing parameter ( $r_1 = r_2 = r_3$ ). In experiments, the requirement is easily achieved by adjusting the two nondegenerate optical parametric amplifiers (NOPAs) to operate at totally same conditions. For our experimental system, we have  $r = 0.4$ .

## B. Covariance matrix of the tripartite optical beams

Gaussian state is the state with Gaussian characteristic functions and quasi-probability distributions on the multi-mode quantum phase space, which can be completely characterized by a covariance matrix. The elements of the tripartite covariance matrix are  $\sigma_{ij} = Cov(\hat{R}_i, \hat{R}_j) = \frac{1}{2} \langle \hat{R}_i \hat{R}_j + \hat{R}_j \hat{R}_i \rangle - \langle \hat{R}_i \rangle \langle \hat{R}_j \rangle$ ,  $i, j = 1, 2, \dots, 6$ , where  $\hat{R} = (\hat{x}_A, \hat{p}_A, \hat{x}_B, \hat{p}_B, \hat{x}_C, \hat{p}_C)^T$  is a vector composed by the amplitude and phase quadratures of tripartite optical beams [42]. Thus covariance matrix of tripartite optical beams can be partially expressed as (the cross correlations between different quadratures are taken as 0)

$$\begin{aligned} \sigma_A &= \begin{bmatrix} \Delta^2 \hat{x}_A & 0 \\ 0 & \Delta^2 \hat{p}_A \end{bmatrix}, \\ \sigma_B &= \begin{bmatrix} \Delta^2 \hat{x}_B & 0 \\ 0 & \Delta^2 \hat{p}_B \end{bmatrix}, \\ \sigma_C &= \begin{bmatrix} \Delta^2 \hat{x}_C & 0 \\ 0 & \Delta^2 \hat{p}_C \end{bmatrix}, \\ \sigma_{AB} &= \begin{bmatrix} Cov(\hat{x}_A, \hat{x}_B) & 0 \\ 0 & Cov(\hat{p}_A, \hat{p}_B) \end{bmatrix}, \\ \sigma_{AC} &= \begin{bmatrix} Cov(\hat{x}_A, \hat{x}_C) & 0 \\ 0 & Cov(\hat{p}_A, \hat{p}_C) \end{bmatrix}, \\ \sigma_{BC} &= \begin{bmatrix} Cov(\hat{x}_B, \hat{x}_C) & 0 \\ 0 & Cov(\hat{p}_B, \hat{p}_C) \end{bmatrix}. \end{aligned} \quad (11)$$

To partially reconstruct all relevant entries of its associated covariance matrix we perform 12 different measurements on the output optical modes. These measurements include the amplitude and phase quadratures of the output optical modes, and the cross correlations  $\Delta^2(\hat{x}_A - \hat{x}_B)$ ,  $\Delta^2(\hat{x}_A - \hat{x}_C)$ ,  $\Delta^2(\hat{x}_B - \hat{x}_C)$ ,  $\Delta^2(\hat{p}_A + \hat{p}_B)$ ,  $\Delta^2(\hat{p}_A + \hat{p}_C)$  and  $\Delta^2(\hat{p}_B + \hat{p}_C)$ . The covariance elements are calculated via the identities [43]

$$\begin{aligned} Cov(\hat{R}_i, \hat{R}_j) &= \frac{1}{2} [\Delta^2(\hat{R}_i + \hat{R}_j) - \Delta^2 \hat{R}_i - \Delta^2 \hat{R}_j], \\ Cov(\hat{R}_i, \hat{R}_j) &= -\frac{1}{2} [\Delta^2(\hat{R}_i - \hat{R}_j) - \Delta^2 \hat{R}_i - \Delta^2 \hat{R}_j]. \end{aligned} \quad (12)$$

In the experiment, we obtain all the covariance matrices of every quantum state actually, and then calculate the PPT value to verify whether the quantum states are entangled or not.

The partially reconstructed covariance matrix of the prepared tripartite entangled optical field is

$$\sigma = \begin{pmatrix} 2.76 & 0 & 2.32 & 0 & 2.27 & 0 \\ 0 & 5.05 & 0 & -2.23 & 0 & -2.27 \\ 2.32 & 0 & 2.78 & 0 & 2.29 & 0 \\ 0 & -2.23 & 0 & 4.81 & 0 & -2.14 \\ 2.27 & 0 & 2.29 & 0 & 2.69 & 0 \\ 0 & -2.27 & 0 & -2.14 & 0 & 4.80 \end{pmatrix}. \quad (13)$$

The entanglement among the prepared tripartite state is evaluated by PPT criterion and we have PPT values  $\text{PPT}_A = 0.48$ ,  $\text{PPT}_B = 0.47$ ,  $\text{PPT}_C = 0.48$ , respectively.

For the tripartite state distributed over lossy (noisy) channels in the experiment we have

$$\begin{aligned}\sigma'_A &= \eta_A \sigma_A + (1 - \eta_A)(g_a N + 1)I, \\ \sigma'_B &= \sigma_B, \\ \sigma'_C &= \eta_C \sigma_C + (1 - \eta_C)I, \\ \sigma'_{AB} &= \sqrt{\eta_A} \sigma_{AB}, \\ \sigma'_{AC} &= \sqrt{\eta_A \eta_C} \sigma_{AC}, \\ \sigma'_{BC} &= \sqrt{\eta_C} \sigma_{BC},\end{aligned}\tag{14}$$

where  $\eta_A$  and  $\eta_C$  are the transmission efficiencies of optical modes  $\hat{A}$  and  $\hat{C}$  respectively,  $N$  and  $g_a$  represent the excess Gaussian noise in the channel and the magnitude of noise respectively. Different combinations of the parameters correspond to different transmission scenarios. When  $\eta_A \neq 1$ ,  $\eta_C \neq 1$  and  $g_a N = 0$ , the optical modes

$\hat{A}$  and  $\hat{C}$  are distributed over two lossy channels, respectively, which corresponds to the scenario shown in Fig. 1(a). If  $\eta_A \neq 1$ ,  $\eta_C = 1$  and  $g_a N = 0$ , only mode  $\hat{A}$  is distributed over a lossy channel, while modes  $\hat{B}$  and  $\hat{C}$  are placed within a node without any channel between them. When the optical mode  $\hat{A}$  is distributed over a noisy channel, the scenario is shown in Fig. 1(b). In this case we have  $\eta_A \neq 1$ ,  $\eta_C = 1$  and  $g_a N \neq 0$ . After the entanglement revival operation, the elements of the covariance matrix for the output state are

$$\begin{aligned}\sigma''_A &= \eta_A T \sigma_A + (1 - \eta_A T)I, \\ \sigma''_B &= \sigma_B, \\ \sigma''_C &= \sigma_C, \\ \sigma''_{AB} &= \sqrt{\eta_A T} \sigma_{AB}, \\ \sigma''_{AC} &= \sqrt{\eta_A T} \sigma_{AC}, \\ \sigma''_{BC} &= \sigma_{BC},\end{aligned}\tag{15}$$

respectively.

- 
- [1] Nielsen, M. A. & Chuang, I. L. *Quantum Computation And Quantum Information*. (Cambridge University, Cambridge, 2000).
- [2] Ralph, T. C. & Lam, P. K. A bright future for quantum communications. *Nat. Photon.* **3**, 671-673 (2009).
- [3] Braunstein, S. L. & van Loock, P. Quantum information with continuous variables. *Rev. Mod. Phys.* **77**, 513-577 (2005).
- [4] Weedbrook, C. *et al.* Gaussian quantum information. *Rev. Mod. Phys.* **84**, 621-669 (2012).
- [5] Raussendorf, R. & Briegel, H. J. A one-way quantum computer. *Phys. Rev. Lett.* **86**, 5188-5191 (2001).
- [6] Walther, P. *et al.* Experimental one-way quantum computing. *Nature* **434**, 169-176 (2005).
- [7] Ukai, R. *et al.* Demonstration of unconditional one-way quantum computations for continuous variables. *Phys. Rev. Lett.* **106**, 240504 (2011).
- [8] Su, X. *et al.* Gate sequence for continuous variable one-way quantum computation. *Nat. Commun.* **4**, 2828 (2013).
- [9] van Loock, P. & Braunstein, S. L. Multipartite entanglement for continuous variables: a quantum teleportation network. *Phys. Rev. Lett.* **84**, 3482-3485 (2000).
- [10] Yonezawa, H., Aoki, T. & Furusawa, A. Demonstration of a quantum teleportation network for continuous variables. *Nature* **431**, 430-433 (2004).
- [11] Jing, J. *et al.* Experimental demonstration of tripartite entanglement and controlled dense coding for continuous variables. *Phys. Rev. Lett.* **90**, 167903 (2003).
- [12] Roslund, J., de Araújo, R. M., Jiang, S., Fabre, C. & Treps, N. Wavelength-multiplexed quantum networks with ultrafast frequency combs. *Nat. Photon.* **8**, 109-112 (2014).
- [13] Pan, J. W., Simon, C., Brukner, Č. & Zeilinger, A. Entanglement purification for quantum communication. *Nature* **410**, 1067 (2001).
- [14] Duan, L. M., Giedke, G., Cirac, J. I. & Zoller, P. Entanglement purification of Gaussian continuous variable quantum states. *Phys. Rev. Lett.* **84**, 4002 (2000).
- [15] Hage, B. *et al.* Preparation of distilled and purified continuous-variable entangled states. *Nat. Phys.* **4**, 915 (2008).
- [16] Dong, R. *et al.* Experimental entanglement distillation of mesoscopic quantum states. *Nat. Phys.* **4**, 919 (2008).
- [17] Yu, T. & Eberly, J. H. Sudden death of entanglement. *Science* **323**, 598-601 (2009).
- [18] Almeida, M. P. *et al.* Environment-induced sudden death of entanglement. *Science* **316**, 579-582 (2007).
- [19] López, C. E., Romero, G., Lastra, F., Solano, E. & Retamal, J. C. Sudden birth versus sudden death of entanglement in multipartite systems. *Phys. Rev. Lett.* **101**, 080503 (2008).
- [20] Aolita, L., Chaves, R., Cavalcanti, D., Acín, A. & Davidovich, L. Scaling laws for the decay of multiqubit entanglement. *Phys. Rev. Lett.* **100**, 080501 (2008).
- [21] Xu, J. S. *et al.* Experimental demonstration of photonic entanglement collapse and revival. *Phys. Rev. Lett.* **104**, 100502 (2010).
- [22] Kim, Y. S., Lee, J. C., Kwon, O. & Kim Y. H. Protecting entanglement from decoherence using weak measurement and quantum measurement reversal. *Nat. Phys.* **8**, 117-120 (2012).
- [23] Yamamoto, N., Nurdin, H. I., James, M. R. & Petersen, I. R. Avoiding entanglement sudden death via measurement feedback control in a quantum network. *Phys. Rev. A* **78**, 042339 (2008).
- [24] Barbosa, F. A. S. *et al.* Robustness of bipartite Gaussian entangled beams propagating in lossy channels. *Nat. Photon.* **4**, 858-861 (2010).
- [25] Coelho, A. S. *et al.* Three-color entanglement. *Science* **326**, 823-826 (2009).
- [26] Kretschmann, D. & Werner, R. F. Quantum channels



- with memory. *Phys. Rev. A* **72**, 062323 (2005).
- [27] Corney, J. F. *et al.* Many-Body Quantum dynamics of polarization squeezing in optical fibers. *Phys. Rev. Lett.* **97**, 023606 (2006).
- [28] Lassen, M., Berni, A., Madsen, L. S., Filip, R. & Andersen, U. L. Gaussian error correction of quantum states in a correlated noisy channel. *Phys. Rev. Lett.* **111**, 180502 (2013).
- [29] Deng, X. *et al.* Disappearance and revival of squeezing in quantum communication with squeezed state over a noisy channel. *Appl. Phys. Lett.* **108**, 081105 (2016).
- [30] Zhang, Y. *et al.* Experimental generation of bright two-mode quadrature squeezed light from a narrow-band non-degenerate optical parametric amplifier. *Phys. Rev. A* **62**, 023813 (2000).
- [31] R. W. P. Drever *et al.*, Laser phase and frequency stabilization using an optical resonator. *Appl. Phys. B* **31**, 97 (1983).
- [32] Horodecki, M., Horodecki, P., & Horodecki, R. Separability of mixed states: necessary and sufficient conditions. *Phys. Lett. A* **223**, 1-8 (1996).
- [33] Simon, R. Peres-Horodecki separability criterion for continuous variable systems. *Phys. Rev. Lett.* **84**, 2726-2729 (2000).
- [34] Werner, R. F. & Wolf, M. M. Bound entangled Gaussian states. *Phys. Rev. Lett.* **86**, 3658-3661 (2001).
- [35] Adesso, G., Serafini, A. & Illuminati, F. Multipartite entanglement in three-mode Gaussian states of continuous-variable systems: Quantification, sharing structure, and decoherence. *Phys. Rev. A* **73**, 032345(2006).
- [36] Vollmer, C. E. *et al.* Experimental entanglement distribution by separable states. *Phys. Rev. Lett.* **111**, 230505 (2013).
- [37] Barbosa, F. A. S. *et al.* Disentanglement in bipartite continuous-variable systems. *Phys. Rev. A* **84**, 052330 (2011).
- [38] Ralph, T. C. Quantum error correction of continuous-variable states against gaussian noise. *Phys. Rev. A* **84**, 022339 (2011).
- [39] Xiang, G. Y., Ralph, T. C., Lund, A. P., Walk, N. & Pryde, G. J. Heralded noiseless linear amplification and distillation of entanglement. *Nature Photon.* **4**, 316-319 (2010).
- [40] Chrzanowski, H. M. *et al.* Measurement-based noiseless linear amplification for quantum communication. *Nature Photon.* **8**, 333-338 (2014).
- [41] Ulanov, A. E. *et al.* Undoing the effect of loss on quantum entanglement. *Nature Photon.* **9**, 764-768 (2015).
- [42] Adesso, G. & Illuminati, F. *J. Phys. A: Math. Theor.* **40**, 7821 (2007).
- [43] Steinlechner, S., Bauchrowitz, J., Eberle, T. & Schnabel, R. *Phys. Rev. A* **87**, 022104 (2013).